study. Quadrupole mass spectrometric investigations will be required to establish clearly the gas phase stability and fate of $Ti(CO)_6$ and $Ti(N_2)_6$ during boil-off experiments.

Conclusion

The infrared and ultraviolet–visible spectroscopic evidence presented for the highest stoichiometry products of the Ti/CO and Ti/N_2 matrix reactions points emphatically to the existence of $Ti(CO)_6$ and $Ti(N_2)_6$, respectively.

The discovery of these 16-electron complexes can be considered to complete the 17- and 18-electron series $V(CO)_6/Cr(CO)_6$ and $V(N_2)_6/Cr(N_2)_6$ and moreover suggests that the metal atom route should provide a synthetic pathway to the Nb, Ta, Mo, and W analogues. Preliminary experiments with these highly refractory metals in our laboratories indicate that in practice this is indeed the case.[22]

A small molecular distortion away from regular octahedral symmetry for $Ti(CO)_6$ and $Ti(N_2)_6$ is implied from the infrared spectroscopic data. The corresponding UV–visible data, on the other hand, appear to be relatively insensitive to this molecular perturbation. The magnitude and symmetry (tetragonal or trigonal) of this distortion cannot be established from the available data. However, one can tentatively say that it is larger than that observed for $V(CO)_6$ and $V(N_2)_6$.

Acknowledgment. We gratefully acknowledge the financial assistance of the National Research Council of Canada and the Atkinson Foundation. The expert assistance of Professor A. B. P. Lever with the analysis of the electronic spectra is also gratefully appreciated.

Registry No. $Ti(CO)_6$, 61332-66-9; $Ti(N_2)_6$, 61332-67-0.

References and Notes

(1) M. T. Anthony, M. L. H. Green, and D. Young, *J. Chem. Soc., Dalton Trans.*, 1419 (1975).
(2) R. Busby, W. Klotzbücher, and G. A. Ozin, *J. Am. Chem. Soc.*, **98**, 4013 (1976).
(3) H. Huber, T. A. Ford, W. Klotzbücher, E. P. Kündig, M. Moskovits, and G. A. Ozin, *J. Chem. Phys.*, in press.
(4) E. P. Kündig, M. Moskovits, and G. A. Ozin, *Nature (London)*, **254**, 503 (1975).
(5) H. Huber, T. A. Ford, M. Moskovits, G. A. Ozin, and W. Klotzbücher, *Inorg. Chem.*, **15**, 1666 (1976).
(6) P. L. Timms, *Chem. Commun.*, 1033 (1969).
(7) E. P. Kündig and G. A. Ozin, *J. Am. Chem. Soc.*, **96**, 3820 (1974).
(8) K. J. Klabunde and H. F. Efner, *Inorg. Chem.*, **14**, 789 (1975).
(9) H. Huber, T. A. Ford, W. Klotzbücher, and G. A. Ozin, *J. Am. Chem. Soc.*, **98**, 3176 (1976).
(10) (a) W. Klotzbücher, A. B. P. Lever, and G. A. Ozin, *Inorg. Chem.*, in press; (b) T. C. DeVore, *Inorg. Chem.*, **15**, 1315 (1976).
(11) E. P. Kündig, M. Moskovits, and G. A. Ozin, *J. Mol. Struct.*, **14**, 137 (1972).
(12) M. Moskovits and G. A. Ozin, *J. Appl. Spectrosc.*, **26**, 481 (1972).
(13) G. A. Ozin and A. Vander Voet, *Acc. Chem. Res.*, **6**, 313 (1973).
(14) E. P. Kündig, M. Moskovits, and G. A. Ozin, *Angew. Chem., Int. Ed. Engl.*, **14**, 292 (1975).
(15) R. W. G. Wyckoff, "Crystal Structures", Vol. 7, Interscience, New York, N.Y., 1974, p 29.
(16) A. D. Buckingham, *Proc. R. Soc. London, Ser. A*, **248**, 1969 (1958); **255**, 32 (1960); *Trans. Faraday Soc.*, **56**, 763 (1960).
(17) L. Hanlan, H. Huber, E. P. Kündig, B. McGarvey, and G. A. Ozin, *J. Am. Chem. Soc.*, **97**, 7054 (1975).
(18) L. Hanlan, H. Huber, and G. A. Ozin, *Inorg. Chem.*, **15**, 2592 (1976).
(19) I. D. Chawla and M. J. Frank, *J. Inorg. Nucl. Chem.*, **32**, 555 (1970).
(20) C. J. Ballhausen, "Introduction to Ligand Field Theory", McGraw-Hill, New Uork, N.Y., 1962.
(21) H. B. Gray and N. A. Beach, *J. Am. Chem. Soc.*, **85**, 2922 (1963).
(22) W. Klotzbücher and G. A. Ozin, in progress.
(23) For consistency the average CO stretching frequency for the doublet splitting in CO/Ar $\simeq$ 1/10 matrices has been used in Figure 7.
(24) Weaker NN stretching modes, whose absorbances were found to be Ti concentration dependent, were observed at higher frequencies (2264/2256 cm^{-1}) than those of VI′ and moreover were found to grow in relation to those of VI′ during matrix warm-up experiments in the range 10–35 K. By analogy with the $V(CO)_6/V_2(CO)_{12}$ and $Ti(CO)_6/Ti_2(CO)_n$ systems, the 2264/2256-cm^{-1} absorptions are probably best ascribed to binuclear or higher titanium cluster dinitrogen species.
(25) The increase in $10Dq$ on passing from $V(N_2)_6$ to $Cr(N_2)_6$ is not so pronounced; see ref 10a.

Contribution No. 5447 from the Arthur Amos Noyes Laboratory of Chemical Physics, California Institute of Technology, Pasadena, California 91125

Studies of the Polarization Behavior, Temperature Dependence, and Vibronic Structure of the 23 000-cm^{-1} Absorption System in the Electronic Spectra of $Mo_2(O_2CCH_3)_4$ and Related Compounds. Emission Spectrum of $Mo_2(O_2CCF_3)_4$ at 1.3 K

WILLIAM C. TROGLER, EDWARD I. SOLOMON, IB TRAJBERG, C. J. BALLHAUSEN, and HARRY B. GRAY*[1]

Received October 17, 1976 AIC607332

The 23 000-cm^{-1} absorption band in the electronic spectrum of $Mo_2(O_2CCH_3)_4$ is primarily polarized perpendicular to the metal–metal axis. Rich vibronic structure is observed for this absorption system in the spectra of $Mo_2(O_2CCH_3)_4$, $Mo_2(O_2CCD_3)_4$, $Mo_2(O_2CCF_3)_4$, and $Mo_2(O_2CH)_4$ at 15 K. Analysis of the temperature dependence of the hot bands in the spectrum of $Mo_2(O_2CCF_3)_4$ has established that the transition is vibronic, being allowed primarily by an a_{2u}(MoMoO) bending vibration ($\sim$190 cm^{-1}). Interpretation of the vibronic structure in the spectrum of $Mo_2(O_2CCH_3)_4$ suggests that the 0–0 transition is split by 275 cm^{-1} into x- and y-polarized components. This splitting, which is much larger in $Mo_2(O_2CCF_3)_4$, correlates with departures from ideal D_{4h} symmetry that are evident from crystal structure determinations. A dominant progression in the MoMo totally symmetric stretch is observed on each of several vibronic origins in the spectrum of $Mo_2(O_2CCH_3)_4$. Franck–Condon analysis demonstrates that a 0.1-Å elongation of the MoMo bond occurs in the excited state. From the lowest energy vibronic origin in $Mo_2(O_2CCF_3)_4$, an estimate of 90 cm^{-1} for the metal–metal torsional frequency is obtained. Structured emission is observed for $Mo_2(O_2CCF_3)_4$ at 1.3 K ($\tau \approx 2$ ms). The emission origin lies 1800 cm^{-1} lower than that of the absorption system. The results are consistent with the assignment of the absorption band to the orbitally forbidden, metal-localized transition $^1A_{1g} \rightarrow {}^1E_g$ ($\delta \rightarrow \pi^*$) and the emission to the corresponding triplet $\rightarrow$ singlet transition.

Introduction

It is now well established that the low-energy absorption system of moderate intensity ($\epsilon \sim 10^3$) in the electronic spectra of $Re_2Cl_8^{2-}$, $Re_2Br_8^{2-}$, $Re_2Cl_6[P(C_2H_5)_3]_2$, and $Mo_2Cl_8^{4-}$ is attributable to the electric dipole allowed transition $\delta \rightarrow \delta^*$ ($^1A_{1g} \rightarrow {}^1A_{2u}$).[2-4] By contrast, spectra of $Mo_2(O_2CR)_4$ (R $\neq$ aromatic) exhibit only a weak low-energy band ($\epsilon \sim 10^2$) which peaks at about 440 nm ($\sim$23 000 cm^{-1}).[5] Recently, Cotton, Martin, and co-workers have examined the polarized crystal spectra of $Mo_2(O_2CCH_2NH_3)_4(SO_4)_2 \cdot 4H_2O$[6] and $Mo_2(O_2CH)_4$.[7] Although a firm assignment of the weak system was not made, it was shown[6] conclusively that the transition in question in the $Mo_2(O_2CR)_4$-type compounds could not be $\delta \rightarrow \delta^*$ ($^1A_{1g} \rightarrow {}^1A_{2u}$).

We have examined the polarized spectra of a crystal of $Mo_2(O_2CCH_3)_4$ as well as films of $Mo_2(O_2CCD_3)_4$,

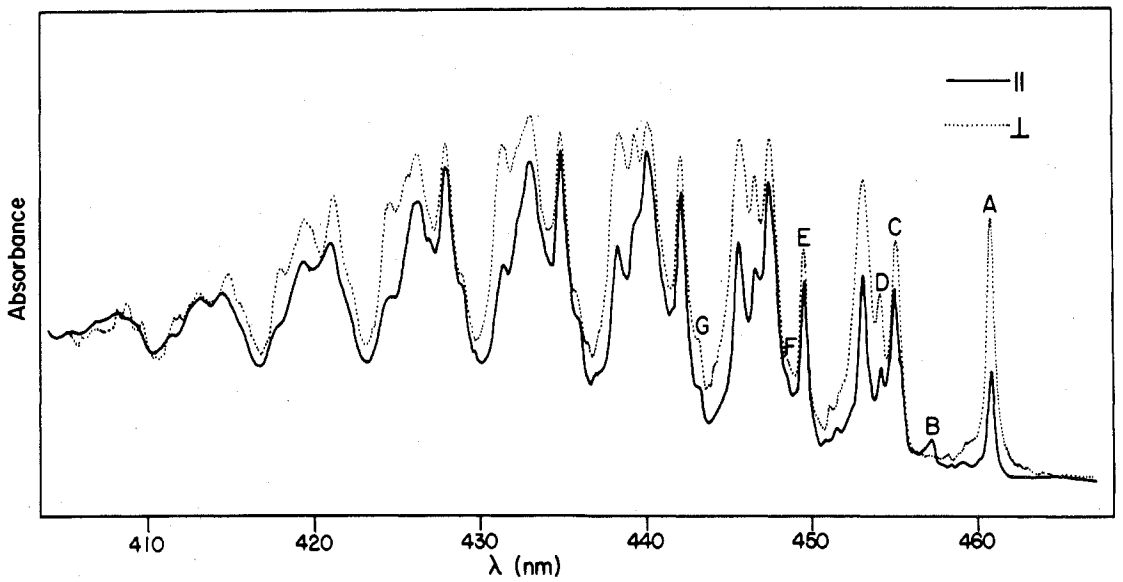

Figure 1. Single-crystal polarized spectra of $Mo_2(O_2CCH_3)_4$ at 15 K. Polarizations are denoted || and ⊥ to the *b* crystallographic axis on the *bc* crystal face. Spectral bandwidth was 0.07 nm.

$Mo_2(O_2CCF_3)_4$, and $Mo_2(O_2CH)_4$ at 15 K. Particular attention has been paid to the elucidation of the hot bands in the spectra of $Mo_2(O_2CCH_3)_4$ and $Mo_2(O_2CCF_3)_4$. The emission spectrum of $Mo_2(O_2CCF_3)_4$ at 1.3 K has also been measured. Our data suggest that the 23 000-cm^{-1} system in molybdenum(II) acetate is derived from a metal-localized, electric dipole forbidden transition to an excited state of ^1E_g symmetry.

Experimental Section

The compounds $Mo_2(O_2CCH_3)_4$,[8] $Mo_2(O_2CCF_3)_4$,[9] $Mo_2(O_2CH)_4$,[10] and $K_4Mo_2Cl_8$[11] were prepared and purified by standard literature methods. Satisfactory elemental analyses were obtained in all cases. The deuterated complex $Mo_2(O_2CCD_3)_4$ was prepared by suspending 0.6 g (0.93 mmol) of $Mo_2(O_2CCF_3)_4$ in 10 mL of deuterated acetic acid. After warming and stirring of the mixture for 2 h, the pale yellow powder was filtered and washed with ethanol and pentane and dried in vacuo. Anal. Calcd for $Mo_2(O_2CCD_3)_4$: C, 21.83; D, 5.49. Found: C, 21.4; D, 5.2.

Low-energy (100–500 cm^{-1}) infrared spectra were recorded on a Perkin-Elmer 180 spectrometer. Sample temperatures of 40 K were attained in a Cryogenics Technology Model 20 Cryocooler, which was equipped with polyethylene windows. Samples of molybdenum(II) carboxylates for the low-energy IR spectra were Vaseline mulls spread on a thin polyethylene disk. Infrared spectra in the range 300–4000 cm^{-1} were recorded on samples in KBr pellets using a Perkin-Elmer 225 instrument. All samples were prepared under a nitrogen atmosphere. Electronic spectra were recorded on a Cary 17 spectrometer. Low temperatures (15 or 80 K) were obtained with a Cary liquid helium Dewar. Temperature was monitored with a calibrated carbon resistor next to the sample on the cooling block. The temperature-dependence study was performed by allowing controlled increases from 80 to 300 K over a 5-h period. Spectra of $Mo_2(O_2CCH_3)_4$, $Mo_2(O_2CCF_3)_4$, $Mo_2(O_2CH)_4$, and $Mo_2(O_2CCD_3)_4$ were obtained from sublimed films on Optasil quartz disks ($^1/_2$-in. diameter; $^1/_{32}$ in. thick) that were mounted in the Dewar using heat-conducting copper grease for good thermal contact. Pellet spectra (KBr) were also recorded and resembled the film spectra but were of lower quality. Slit width and lamp settings were such that a spectral bandwidth of less than 0.07 nm was maintained for all low-temperature optical spectra. The emission spectrum was measured at 1.3 K, obtained by pumping on liquid helium in an optical Dewar. A pulsed nitrogen laser (337 nm) was used to excite the sample whose emission was recorded at 0.6-nm resolution using boxcar integration techniques. The spectrum was corrected for phototube response before plotting.

Both $Mo_2(O_2CCH_3)_4$[12] and $Mo_2(O_2CCF_3)_4$[9] crystallize in the triclinic space group $P\bar{1}$. Crystals of reasonable size were obtained only for $Mo_2(O_2CCH_3)_4$. The needlelike crystals were observed to grow with two kinds of well-formed faces. These types were readily distinguished, as one face exhibited extinction directions nearly parallel (within 2°) and perpendicular to the needle axis, whereas the extinction directions for the other face made an approximately 15° angle with the needle axis. Polarized spectra were recorded for the former type of crystal face. Subsequent x-ray oscillation, Weissenberg, and precession photographs showed conclusively that the needle axis was the crystallographic *b* axis and that polarized spectra were taken parallel and perpendicular to *b* within 10° of the *bc* crystal face.

Polarization ratios were calculated for transitions assumed to be polarized along the MoMo (*z*) and the mutually perpendicular MoO (*x*, *y*) axes. These calculations were performed by projecting the molecular axes along the extinction directions. Adopting the same notation used in the crystal structure analysis,[12] we report the following polarization ratios $\|b/\perp b$ for the *bc* crystal face: $z = 3.61$, $x = 0.004$ (MoO(1), 0.008; MoO(3), 0.000), $y = 0.55$ (MoO(2), 0.618; MoO(4), 0.476). The calculations show that the assumption that the principal absorption directions lie along the MoMo and MoO axes does not hold rigorously for the molecule in the low-symmetry crystal environment, and we emphasize that uncertainties are to be associated with the reported polarization ratios; nevertheless, the calculations are entirely consistent with the observation of strong parallel and both strong and weak perpendicularly polarized features.

The oscillator strength of the 23 000-cm^{-1} band in $Mo_2(O_2CCF_3)_4$ was determined from measurements on an oxygen-free acetonitrile solution at room temperature. From a plot of the spectrum on an energy scale, the oscillator strength was found by cut-and-weight integration of the peak, allowing for the overlapping tails of intense bands at 297 and 335 nm. For $K_4Mo_2Cl_8$, a freshly prepared, degassed (10 °C, 6 N HCl) solution was employed to obtain an oscillator strength.

Results and Discussion

The oscillator strength of the 22 700-cm^{-1} band in the absorption spectrum of $Mo_2(O_2CCF_3)_4$ in acetonitrile solution at 298 K is 0.0011. This value is an order of magnitude less than that (0.015)[13] obtained for the $\delta \rightarrow \delta^*$ band at 19 300 cm^{-1} in $K_4Mo_2Cl_8$. Examination of the spectra of $Mo_2(O_2CCF_3)_4$ and $Mo_2(O_2CH)_4$ at 40 K between 4000 and 22 000 cm^{-1} revealed no lower energy electronic bands of appreciable intensity ($\epsilon > 10$). Upon cooling, the 23 000-cm^{-1} band in each of four complexes ($Mo_2(O_2CCH_3)_4$, $Mo_2(O_2CCD_3)_4$, $Mo_2(O_2CCF_3)_4$, and $Mo_2(O_2CH)_4$[7]) shows remarkable vibronic structure (Figures 1, 2; Tables I–IV). The integrated intensity of this band increases slightly (10–15%) and a red shift is exhibited between 15 and 300 K. It is unlikely that the weak band represents a spin-forbidden transition, as a similarly structured emission system ($\tau = 2$ ms) was observed at lower energy (0–0 gap of 1800 cm^{-1}) in a film of

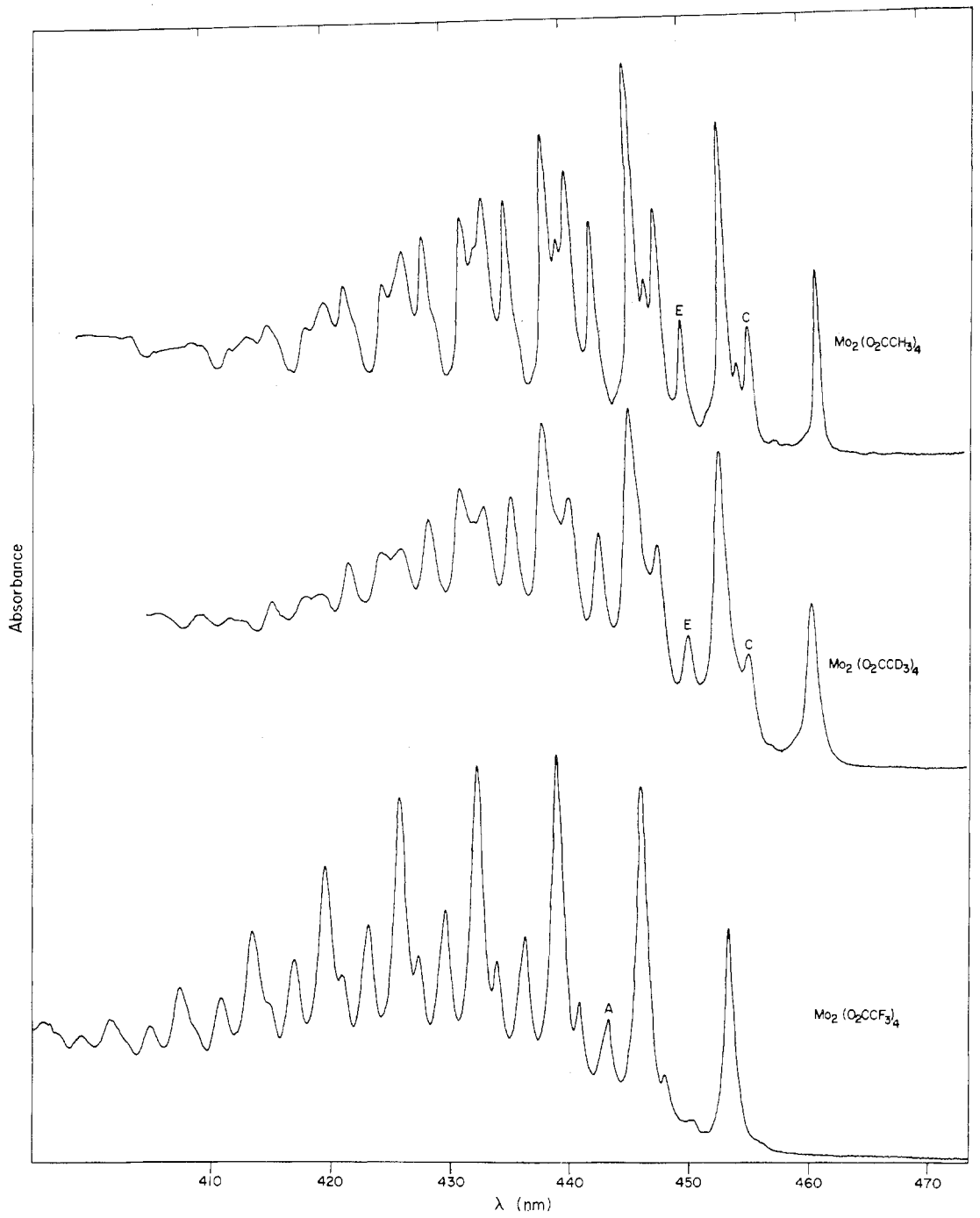

Figure 2. Electronic spectra of $Mo_2(O_2CCH_3)_4$, $Mo_2(O_2CCD_3)_4$, and $Mo_2(O_2CCF_3)_4$ at 15 K. Spectra of sublimed films on quartz disks at 0.07-nm bandwidth were recorded.

$Mo_2(O_2CCF_3)_4$ at 1.3 K (Figure 3; Table V). From the oscillator strength of the absorption band, a radiative lifetime of 2 μs is estimated.[14] Therefore, the long-lived emission is logically assigned to a transition from the triplet state that is related to the singlet excited in absorption at 23 000 cm^{-1}. The $Mo_2(O_2CCH_3)_4$ complex does not emit, which may reflect the more efficient radiationless processes expected for a molecule possessing high-frequency (CH) vibrations in the weak coupling limit.[15]

Upon examination of the low-energy side of the first intense vibronic component in the spectrum of $Mo_2(O_2CCF_3)_4$ (22 064 cm^{-1}; A, Figure 4), by using a thick sample, additional weak features were observed at 21 950 and 21 862 cm^{-1} (B, C, Figure 4). At 15 K these weak features cannot be hot bands on the 22 064-cm^{-1} "origin", as their intensities are several orders of magnitude too large. This observation implies that there must be a lower energy forbidden origin. When the temperature is increased to 80 K, hot bands (D, E, Figure 4) are exhibited at 21 773 and 21 671 cm^{-1}. The temperature dependence of the latter hot band is clearly resolved over a large temperature range (80–260 K), whereas the 21 773-cm^{-1} hot band was obscured by broadening of the more intense 22 064-cm^{-1} component at higher temperatures. As a hot band arises from thermal population of ground-state vibrations, its temperature-dependent intensity should follow a Boltzmann distribution. In Figure 5 the Boltzmann plot for the 21 671-cm^{-1} hot band is shown. The slope obtained corresponds to a ground-state vibrational spacing of 206 ± 20 cm^{-1}. This means that the hot band is built on a weak electronic origin (i.e., the true 0–0 energy for the transition) approximately midway between 21 671 cm^{-1} and the first intense vibronic component (22 064 cm^{-1}) of the transition. In fact, a weak feature is

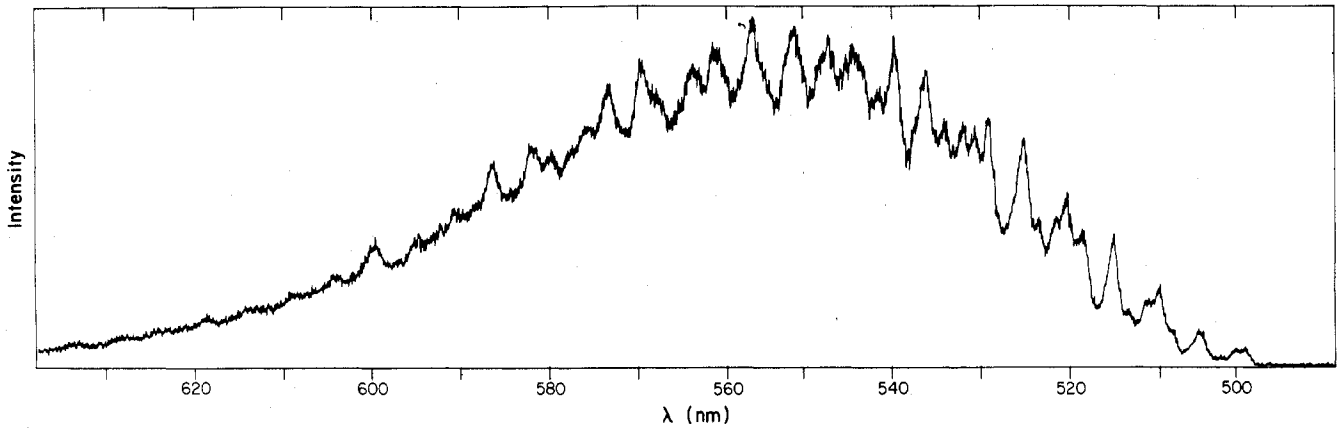

Figure 3. Corrected emission spectrum of a thick sublimed film of $Mo_2(O_2CCF_3)_4$ on quartz at 1.3 K. The sample was irradiated at 337 nm with a pulsed nitrogen laser and the spectrum was recorded at 0.6-nm bandwidth.

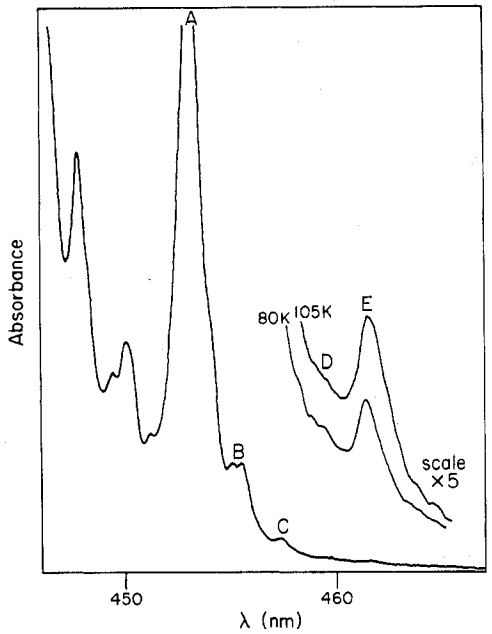

Figure 4. Band origin in the electronic spectrum of $Mo_2(O_2CCF_3)_4$ at 15 K. Hot bands (80 and 150 K) are shown at a vertical scale expansion of 5. The spectra were recorded at 0.07-nm bandwidth.

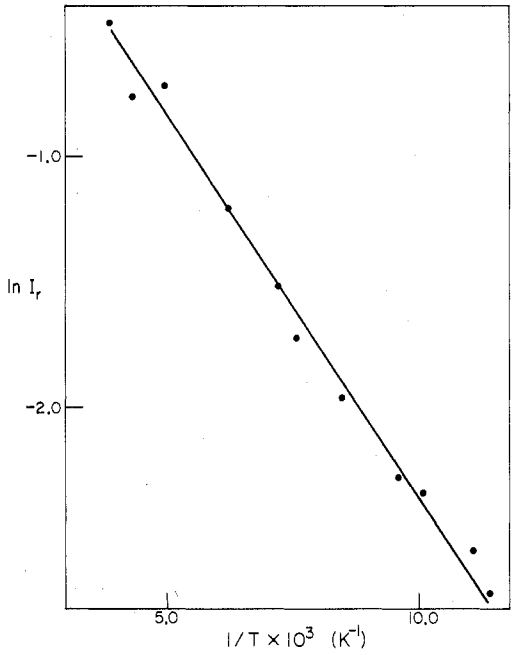

Figure 5. Boltzmann plot of the temperature dependence of the hot-band intensity (I_r) for $Mo_2(O_2CCF_3)_4$.

observed at 21 862 cm^{-1} (C, Figure 4), where the hot-band analysis predicts the 0–0 transition to occur. Moreover, the intensity of this weak peak is temperature independent (observable between 15 and 80 K), ruling out its assignment to a low-frequency, vibronically allowed transition. Therefore, we conclude that 21 862 cm^{-1} is the 0–0 transition energy and that its intensity is derived from magnetic dipole allowedness.[16] The 0–0 feature is about 100 times less intense than the vibronic portion of the system, which places its oscillator strength at about 10^{-5} (a reasonable order of magnitude for a magnetic dipole transition).[17] As will be shown later, the excited state is ^1E_g in D_{4h}, and $^1A_{1g} \rightarrow {}^1E_g$ is allowed as a magnetic dipole transition. Because the crystallographic symmetry is C_i[12] and the 0–0 transition will be shown to be even → even, the electric dipole forbiddenness and magnetic dipole allowedness are rigorous. Similar hot bands are observed in the spectrum of $Mo_2(O_2CCH_3)_4$, and their polarizations are shown in Figure 6. Unfortunately, resolution of the vibronic structure was not sufficient to observe the 0–0 band directly. The 21 302-cm^{-1} hot band (A, Figure 6) and the first vibronic component at 21 696 cm^{-1} (A, Figure 1) are polarized similarly. This provides additional evidence that this hot band and first intense component derive their intensities by coupling the *same* nontotally symmetric vibration (ground state 191 cm^{-1} for the hot band and excited-state energy of 202 cm^{-1} for the first intense component) with an electric dipole forbidden 0–0 transition approximately midway between them. The spectrum of $Mo_2(O_2CH)_4$ also exhibits a similarly behaved hot band ~375 cm^{-1} to lower energy of the first intense peak of the system (Table IV). Therefore, the allowedness of the first vibronic component of the 23 000-cm^{-1} band in $Mo_2(O_2CCH_3)_4$, $Mo_2(O_2CCF_3)_4$, and $Mo_2(O_2CH)_4$ is attributed to coupling with a ~190-cm^{-1} vibration.

An important feature of the polarized spectra (Table I) of $Mo_2(O_2CCH_3)_4$ is the presence of vibronic components with *three* different polarization ratios. For example, the first intense component (A, Figure 1) is *strongly* polarized perpendicular, the weak feature at 21 870 cm^{-1} (C, Figure 7) is polarized parallel, and the intense peaks at 21 969 and 22 244 cm^{-1} (C, E, Figure 1) are *weakly* polarized perpendicular to the metal–metal axis. The presence of two perpendicularly polarized bands (strong and weak) suggests a low-symmetry splitting into x and y components with different polarization ratios, as expected (see Experimental Section), owing to the alignment of the molecule with respect to the crystallographic axes. There are two possible explanations for the low-sym-

Table I. Vibronic Structure of the Lowest Energy Visible Band in the Spectrum of $Mo_2(O_2CCH_3)_4$ at 15 K

nm	cm^{-1}	Polarizn[d]	Assignment[e]
469.44	21 302[a]	⊥s	$\nu_0 - a_{2u}(g)$
466.68	21 428[a]	⊥w	$\nu_0 - a_{1u}(g)$
	21 500[b]		ν_0
460.91	21 695	⊥s	$\nu_0 + a_{2u}$
459.66	21 755[c]	⊥w	$\nu_0 + \Gamma_u$
458.78	21 797[c]	⊥w	$\nu_0 + \Gamma_u$
458.34	21 818[c]	⊥s	$\nu_0 + a_{2u}'$
457.25	21 870	∥	$\nu_0 + e_u$
455.19	21 969	⊥w	$\nu_0' + a_{2u}$
454.19	22 017	⊥s	$\nu_0 + \Gamma_u(OCO)$
453.19	22 066	⊥s	
451.16	22 165	⊥w	
449.56	22 244	⊥w	$\nu_0' + \Gamma_u(OCO)$
448.69	22 287	⊥w	$\nu_0' + a_{2u} + a_{1g}$
447.51	22 346	⊥w	
446.61	22 391	⊥s	
445.71	22 436	⊥s	
443.18	22 564	⊥w	$\nu_0' + \Gamma_u(OCO) + a_{1g}$
442.13	22 618	⊥w	
441.00	22 676	⊥w	
440.18	22 718	⊥w	
439.23	22 767	⊥s	
438.29	22 816	⊥s	
435.81	22 946	⊥w	
434.84	22 997	⊥w	
433.05	23 092	⊥w	
431.35	23 183	⊥s	
429.00	23 310	⊥w	
427.88	23 371	⊥w	
426.24	23 461	⊥w	
424.59	23 552	⊥s	
422.42	23 673	⊥w	
421.25	23 739	⊥w	
419.46	23 840	⊥w	
418.01	23 923	⊥s	

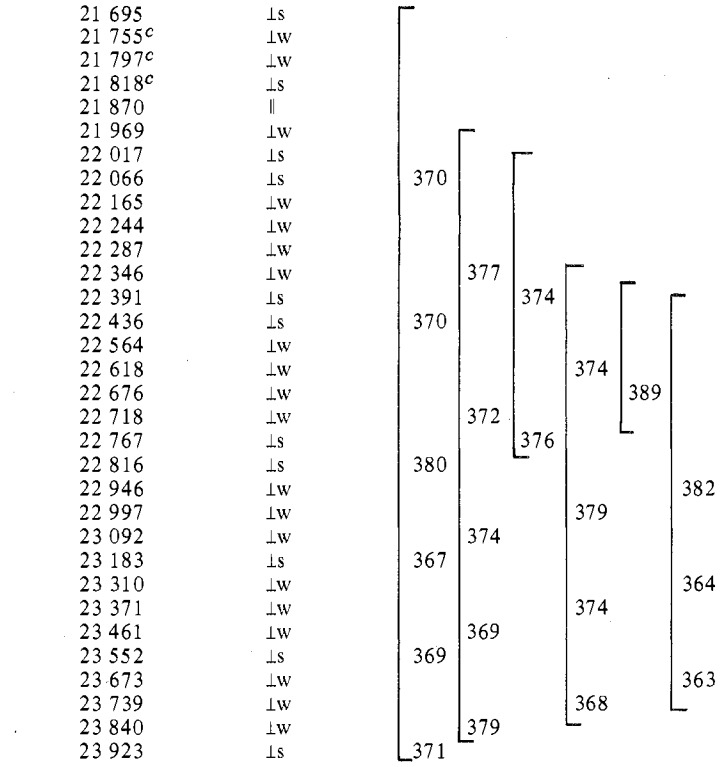

[a] Hot bands were not detected at 15 K but were evident in a thick crystal at 80 K. [b] 0-0 energy estimated from the hot band (but not observed in the spectrum). [c] Weak features observed in a thick crystal at 15 K. [d] ∥ denotes polarization along the MoMo axis. ⊥w signifies weak polarization perpendicular to the MoMo axis. ⊥s signifies strong polarization perpendicular to the MoMo axis. [e] Only the origins for progressions in the totally symmetric MoMo stretch are shown since higher members of the progression are indicated by the numbered bars. The ground-state MoMoO bending mode is $a_{2u}(g)$, and $a_{1u}(g)$ is the corresponding metal-metal torsional vibration. The two pure electronic origins are denoted by ν_0 and ν_0'. Excited-state MoO stretching modes are a_{2u}', e_u, and a_{1g}, and a_{2u} is an excited-state MoMoO bending mode. An excited-state antisymmetric carboxylate deformation is $\Gamma_u(OCO)$, and $\nu_0 + \Gamma_u$ denotes an unassigned vibronic origin.

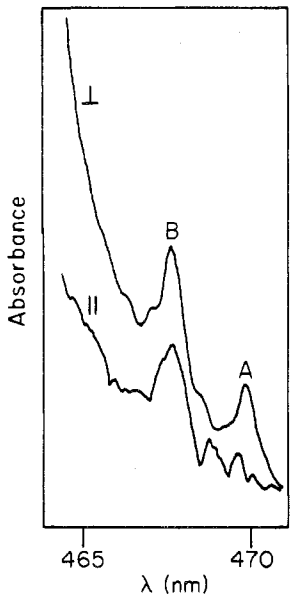

Figure 6. Hot bands in the single-crystal polarized spectra of $Mo_2(O_2CCH_3)_4$ at 80 K. Polarizations are denoted ∥ and ⊥ to the *b* crystallographic axis on the *bc* face.

metry splitting. If the excited state involved in the forbidden transition were orbitally degenerate (i.e., ^1E_g) in D_{4h} symmetry, then in the C_i site of the crystal a splitting of the electronic origin would occur, producing two different components with *x* and *y* polarization ratios (a Davydov splitting can be ruled out, as there is only one molecule in the unit cell[12]). Alternatively, the split transition could arise as a result of a nondegenerate electronic excited state ($^1A_{1g}(u)$, $^1A_{2g}$, $^1B_{1g}(u)$, or $^1B_{2g}(u)$) coupling with a low-symmetry-split $e_u(g)$ *vibration* of the molecule. To investigate the latter possibility, we have examined the infrared spectra of mulls of $Mo_2(O_2CCH_3)_4$, $Mo(O_2CCF_3)_4$, and $Mo_2(O_2CH)_4$ in the 100–500-cm^{-1} region at 40 K. An intense band system centered at 360 cm^{-1} is exhibited in the spectrum of $Mo_2(O_2CCH_3)_4$. This system is split by 25 cm^{-1} into a sharp component at 372 cm^{-1} and a somewhat broader one at 347 cm^{-1}. Force constant calculations[18] have shown that this intense system arises from the IR-active a_{2u} and e_u MoO stretching vibrations. The broader band, which presumably represents the e_u vibration, has a line width of ca. 30 cm^{-1}. Bands were also observed in the MoMoO bending region at 175 and 228 cm^{-1} for $Mo_2(O_2CCH_3)_4$, at 170 and 232 cm^{-1} for $Mo_2(O_2CH)_4$, and at 190 and 216 cm^{-1} for $Mo_2(O_2CCF_3)_4$. Force constant calculations for $Mo_2(O_2CCH_3)_4$ have suggested that these bands are attributable to a_{2u} and e_u MoMoO bending vibrations.[18] As none of the e_u vibrations is split sufficiently to explain the separation of the *x*- and *y*-polarized vibronic components, the electronic transition must be to a split ^1E_g state. Of interest is the fact that all three compounds show a vibrational band in the energy range (170–190 cm^{-1}) where the hot-band analysis placed the vibronically active fundamental for the first intense origin. Our analysis suggests an

Table II. Vibronic Structure of the Lowest Energy Visible Band in the Spectrum of $Mo_2(O_2CCF_3)_4$ at 15 K

nm	cm^{-1}					Assignment[e]
461.45	21 671[a]					$\nu_0 - a_{2u}(g)$
459.28	21 773[a]					$\nu_0 - a_{1u}(g)$
457.41	21 862[b,c]					ν_0
455.58	21 950[b]					$\nu_0 + a_{1u}$
455.10	21 973[b]					$\nu_0 + \Gamma_u$
453.23	22 064					$\nu_0 + a_{2u}$
451.22	22 162[b]					$\nu_0 + \Gamma_u$
450.11	22 217[b]					$\nu_0 + \Gamma_u$
449.46	22 249[b]					$\nu_0 + \Gamma_u$
447.89	22 327					$\nu_0 + \Gamma_u(OCO)$
445.93	22 425	361				
443.16	22 565[d]				348	$\nu_0 + a_{2u} + a_{1g}$
440.70	22 691		364			
438.77	22 791	366				
436.17	22 927				362	
433.86	23 049		358			
432.10	23 143	352				
429.50	23 283				356	
427.30	23 403		354			
425.68	23 492	349				
423.08	23 636				353	
420.86	23 761		358			
419.46	23 840	348				
416.91	23 986				350	
415.00	24 096		335			
413.36	24 192	352				
410.83	24 341				355	
408.76	24 464		368			
407.35	24 549	357				
404.87	24 699				358	

[a] Hot bands were not detected at 15 K but were evident at 80 K in a thick sample. [b] Weak bands observed in thick path length sample. [c] 0–0 band observed in the spectrum and confirmed as such by the hot-band temperature dependence. [d] This band is broad with a distinct high-energy shoulder and remains as such throughout the progression, indicating two overlapping weak progressions. [e] Notation as in Table I; a_{1u} is an excited-state metal-metal torsional vibration.

Table III. Vibronic Structure of the Lowest Energy Visible Band in the Spectrum of $Mo_2(O_2CCD_3)_4$ at 15 K

nm	cm^{-1}					Assignment[a]
460.29	21 725					$\nu_0 + a_{2u}$
456.76	21 893					$\nu_0 + e_u$
454.94	21 981					$\nu_0' + a_{2u}$
452.59	22 095	370				
449.76	22 234					$\nu_0' + \Gamma_u(OCO)$
447.29	22 357		376			
445.00	22 472	377				
442.35	22 606				372	
440.00	22 727		370			
437.82	22 840	368				
435.14	22 981				375	
432.94	23 098		371			
430.88	23 208	368				
428.26	23 350				369	
426.11	23 468		370			
424.41	23 562	354				
421.59	23 720				370	
419.29	23 850		382			
418.12	23 917	355				
415.17	24 087				367	

[a] Notation as in Table I.

a_{2u} assignment for this band, as a_{2u} would induce x- and y-polarized components in a transition to a split ^1E_g state, according to the Herzberg–Teller coupling scheme.[19]

The vibrational fine structure of the 23 000-cm^{-1} band may be assigned after proper account is taken of the following. As the pure electronic transition is forbidden, all of the strong features at 15 K must arise from excitation of a quantum of one of several possible antisymmetric vibrations in the excited state (Table VI). A progression of spacing 355–370 cm^{-1} is built on each vibronic origin (three strong ones for $Mo_2(O_2CCH_3)_4$ and only one for $Mo_2(O_2CCF_3)_4$). Weak features pose a problem, as they can be either new vibronic origins or progressions on one of the intense vibronic bands with a small Franck–Condon factor. For example, if the Franck–Condon factor is 0.4, a progression with relative intensities of 1:0.4:0.08:0.01... is expected. Therefore, in a complex spectrum, only the first two bands would be observable.

Only one dominant progression, which must represent quanta of a totally symmetric vibration, is exhibited by $Mo_2(O_2CCF_3)_4$ (ca. 355 cm^{-1}) and $Mo(O_2CCH_3)_4$ (ca. 370 cm^{-1}). There are only two a_{1g} modes of the Mo_2O_8 unit that

Table IV. Vibronic Fine Structure of $Mo_2(O_2CH)_4$ at 15 K

nm	cm^{-1}					Assignment[e]
465.27[a]	21 493					$\nu_0 - a_{2u}(g)$
457.29	21 868					$\nu_0 + a_{2u}$
456.79	21 892					
456.50[b]	21 906					
454.65	21 995					
451.94	22 127					
451.21[b]	22 163					
449.82[b]	22 231	363				
449.26	22 259					
c						
448.33[b]	22 305					
447.53[b]	22 345					
444.80[b]	22 482					
444.08	22 518					
442.88[b]	22 579	348				
442.16[b]	22 616					
441.45	22 653					
440.53	22 700					
436.29[d]	22 920					
429.59[d]	23 278					
423.06[d]	23 637					
416.71[d]	23 997					
410.71[d]	24 350					
405.18[d]	24 680					

[a] Broad hot band observed at 80 K. [b] Shoulder. [c] Not resolved. [d] Maximum of a broad peak that contains many unresolved components. [e] Notation as in Table I.

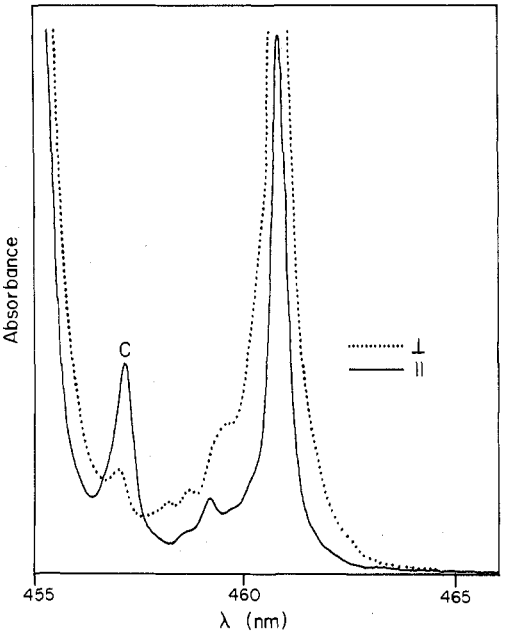

Figure 7. Weak features in the single-crystal polarized spectra of $Mo_2(O_2CCH_3)_4$. Polarizations are denoted || and ⊥ to the b crystallographic axis on the bc face. The spectra were recorded at 15 K with 0.07-nm bandwidth.

Table V. Vibronic Structure in the Emission Spectrum of $Mo_2(O_2CCF_3)_4$ at 1.3 K

nm	cm^{-1}					
498.80	20 048					
499.73	20 011					
501.61	19 936					
503.88	19 846					
506.95	19 726					
508.57	19 663	385				
509.92	19 611		400			
512.11	19 527			409		
513.82	19 462				384	
517.41	19 327					399
519.61	19 262	401				
520.51	19 212		399			
522.55	19 137			390		
524.27	19 074				388	
528.26	18 930					397
529.80	18 875	387				
531.26	18 823		389			
533.28	18 752			385		
535.62	18 670				404	
538.94	18 555					375
540.98	18 485	390				
542.62	18 429		394			
544.25	18 374			378		
546.78	18 289				381	
547.41	18 268					
550.60	18 162					393
	Obscured	378				
554.08	18 048		381			
555.56	18 000			374		
558.47	17 906				383	
559.79	17 864					404
562.46	17 779					
564.02	17 730	378				
566.70	17 646		402			
568.41	17 593			407		
572.18	17 477					387
574.38	17 410					
576.27	17 353	377				
578.87	17 275		371			
580.89	17 215			378		
585.58	17 077					400
587.54	17 020					
590.07	16 947		389			
594.32	16 826			389		
599.88	16 670					407

Table VI. Vibronic Intensity Inducing Vibrations ($^1A_{1g}$ Ground State)

Polarizn direction	Excited states		
	D_{4h} symmetry	D_{2h} symmetry	
	^1E_g state	$^1B_{2g}$ state	$^1B_{3g}$ state
x	a_{1u}		a_u
	a_{2u}	b_{1u}	
	b_{1u}		a_u
	b_{2u}	b_{1u}	
y	a_{1u}	a_u	
	a_{2u}		b_{1u}
	b_{1u}	a_u	
	b_{2u}		b_{1u}
z	e_u	b_{3u}	b_{2u}

fall in this energy region. Bands attributable to the a_{1g} (MoMo) stretch were observed in the Raman spectra of $Mo_2(O_2CCH_3)_4$ (406 cm^{-1})[18] and $Mo_2(O_2CCF_3)_4$ (397 cm^{-1}).[9] A Raman peak also was observed[20] at 322 cm^{-1} for $Mo_2(O_2CCH_3)_4$, where force constant calculations place a_{1g}(MoO).[18] As the average MoO bond length in $Mo_2(O_2CCF_3)_4$ is shorter than that in $Mo_2(O_2CCH_3)_4$ (vide infra), we would expect the a_{1g}(MoO) stretch to occur at higher energy in the former complex; however, the progressional energies display the opposite trend. For this reason, the spacings of 355 and 370 cm^{-1} are logically attributable to an excited-state a_{1g}(MoMo) stretch that is reduced somewhat from the ground-state value. The emission system of $Mo_2(O_2CCF_3)_4$ exhibits one major progression with a spacing of ca. 390 cm^{-1}, which is in good agreement with the Raman band at 397 cm^{-1} assigned to a_{1g}(MoMo).[9]

A progression in the metal–metal stretching frequency reflects a displacement of the excited-state geometry from the ground state along this normal coordinate. The intensity I_n of the nth member of a vibrational progression is given by the Poisson distribution[21]

$$I_n = I_0 S^n / n!$$

The Franck–Condon factor S is most simply obtained from the ratio I_1/I_0. This is related to the distortion, Q_0^{α}, from equilibrium along an a_{1g} mode of frequency ω_α by

$$S = (1/2)k(Q_0^{\alpha})^2/h\omega_\alpha$$

Force constant calculations on $Mo_2(O_2CCH_3)_4$ have given $k_{MoMo} \simeq 3.73$ mdyn/Å for the 406-cm^{-1} a_{1g} mode (~75% MoMo stretching).[18] Using these parameters and a value $S = 2.2$ obtained from the electronic spectrum, we calculate $Q_0^{MoMo} \simeq 0.1$ Å.

As mentioned above, the most intense vibronic component is allowed by coupling the 0–0 transition with an a_{2u} vibration. In the ground state, the a_{2u}(MoMoO) vibrational quantum for $Mo_2(O_2CCF_3)_4$ is 191 cm^{-1}, and similar values are found for $Mo_2(O_2CCH_3)_4$ and $Mo_2(O_2CH)_4$. According to vibronic selection rules (Table VI), either an a_{1u}, a_{2u}, b_{1u}, or b_{2u} mode can induce perpendicularly polarized intensity into $^1A_{1g} \rightarrow {}^1E_g$. If we assume that the molecular symmetry is reduced to D_{2h}, we note that a_{1u} and b_{1u} (a_{2u} and b_{2u}) correlate with an a_u (b_{1u}) vibration, which induces x (y) polarization in the $^1A_g \rightarrow {}^1B_{2g}$ component of the parent $^1A_{1g} \rightarrow {}^1E_g$ transition and y (x) polarization in $^1A_g \rightarrow {}^1B_{3g}$, thereby accounting for the observed behavior. The a_{1u} metal–metal torsional vibration is expected to be of low frequency. In fact, the lowest energy weak feature (21 950 cm^{-1}; B, Figure 4) in $Mo_2(O_2CCF_3)_4$ might be the a_{1u} vibronic origin, which would place the metal–metal torsional frequency at about 90 cm^{-1}. The related hot band is observed at 21 773 cm^{-1} (D, Figure 4). Polarization of the corresponding feature (21 428 cm^{-1}; B, Figure 6) in $Mo_2(O_2CCH_3)_4$ is consistent with the proposed assignment.

The a_{2u}, b_{1u}, and b_{2u} modes are all MoMoO deformations, calculated to lie near 200 cm^{-1} in $Mo_2(O_2CCH_3)_4$.[18] We favor a_{2u} as the dominant, vibronically active mode, particularly in view of the close agreement between the vibrational quantum derived from the hot band (191 cm^{-1}) and the 190-cm^{-1} peak in the low-temperature IR spectrum of $Mo_2(O_2CCF_3)_4$. The parallel polarized component of low intensity at 21 870 cm^{-1} (or ca. 370 cm^{-1} from the estimated position of the 0–0 band) in the spectrum of $Mo_2(O_2CCH_3)_4$ (C, Figure 7) must represent another vibronic origin (rather than a quantum of an a_{1g} vibration built on 21 696 cm^{-1}). It is likely that coupling with the e_u(MoO) stretching vibration induces the z polarization (ground state 347 cm^{-1}).

A weak band at 21 818 cm^{-1} that is strongly xy polarized in the spectrum of $Mo_2(O_2CCH_3)_4$ is assigned to a transition involving a quantum of a_{2u}(MoO) built upon the 0–0 component at about 21 500 cm^{-1}. The two intense features at 21 969 and 22 244 cm^{-1}, which are polarized weakly perpendicular, are attributed to vibronic origins on the second component of the 0–0 $^1A_{1g} \rightarrow {}^1E_g$ band (vide supra). As the second 0–0 component, unlike the first, could not be located with certainty, definitive assignments are not possible. If we assume that the 21 969-cm^{-1} peak represents a quantum of a_{2u}(MoMoO) built upon the second 0–0 component, then the

low-symmetry splitting of ^1E_g is about 275 cm^{-1} (i.e., second 0–0 at ~21 775 cm^{-1}).

The 22 244-cm^{-1} peak (E, Figure 1) is not a member of an a_{1g} progresssion on either of the intense vibronic origins, because the third member of such a progression is not observed. Therefore, it is a vibronic origin on one of the two 0–0 components, corresponding either to a 469- or a 744-cm^{-1} vibration. Such high energies cannot result from MoO vibrations but must involve a carboxylate ligand deformation that lowers the symmetry of the Mo_2O_8 unit, thereby allowing the transition. Support for this suggestion comes from a comparision with the spectrum of the deuterated complex, $Mo_2(O_2CCD_3)_4$ (Figure 2). Relative to the positions of the other peaks in the spectrum, only the 22 244-cm^{-1} band (E, Figure 2) displays a noticeable red shift (~40 cm^{-1}) in the deuterated complex. Band D (Figure 1) is absent in $Mo_2(O_2CCD_3)_4$, which implies either a low or high energy shift to a position at which it is obscured by a more intense peak (21 981 (C, Figure 2) or 22 095 cm^{-1}).

In IR spectra measured in KBr pellets at ambient temperature, a band attributable to OCO bending shows a similar red shift (675 to 645 cm^{-1}). Although an absorption assignable to the ρ_r(OCO) deformation was not observed in the IR spectrum of $Mo_2(O_2CCH_3)_4$, one such feature occurs at 460 cm^{-1} in acetate ion.[22] Therefore, we assign the 22 244-cm^{-1} peak to a vibronic origin involving a 469-cm^{-1} OCO deformation built on the second 0–0 component. Band D is attributed to a transition involving a similar OCO deformation built on the first 0–0 component. We assume that the apparent absence of band D in the spectrum of $Mo_2(O_2CCD_3)_4$ is due to a 40-cm^{-1} red shift, which results in the weak absorption being buried beneath band C (Figure 2).

Bands F and G (Figure 1), which occur 318 and 320 cm^{-1} above C and E, respectively, are assigned to transitions involving a quantum of the a_{1g}(MoO) stretching vibration built on the two strong vibronic origins. The polarizations of F and G match C and E, as expected, and force constant calculations predict a_{1g}(MoO) to be about 320 cm^{-1} in the ground state.[18] This a_{1g} progression has a small Franck–Condon factor (ca. 0.3) and therefore diminishes according to 1:0.3:0.045. Hence, the third member in the progression would not be observable. The small Franck–Condon factor for the symmetric MoO stretch indicates that the excited-state distortion along that normal coordinate is minimal.

Because no polarization data or force constant calculations for $Mo_2(O_2CCF_3)_4$ are available, the vibrational assignments given in Table II are less certain. Assignments are made by analogy with the interpretation of the spectrum of $Mo_2(O_2CCH_3)_4$. Discussion of the differences in the spectra of $Mo_2(O_2CCH_3)_4$ and $Mo_2(O_2CCF_3)_4$ is facilitated by recalling the reported[9,12] bond distances (Å) in the two complexes, as in

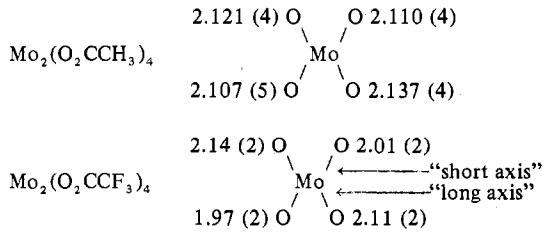

The relative simplicity of the spectrum of $Mo_2(O_2CCF_3)_4$ may be associated with the substantial distortion of the Mo_2O_8 unit from D_{4h} symmetry. Only one strong component is exhibited in the spectrum, and the medium-intensity component (A, Figure 2) actually is comprised of two overlapping weak progressions (Table II). The spectrum of $Mo_2(O_2CCH_3)_4$ exhibits, by contrast, three strong progressional origins of comparable intensity, and band C (Figure 2), which does not red shift appreciably in $Mo_2(O_2CCD_3)_4$ (10 cm^{-1} or less) and which has no counterpart in $Mo_2(O_2CCF_3)_4$, is one of the more intense vibronic features. It is logical to propose that, in the distorted Mo_2O_8 unit of $Mo_2(O_2CCF_3)_4$, one of the components of $^1A_{1g} \rightarrow {}^1E_g$ is moved to higher energy and is buried under more intense peaks, whereas the other component, which is associated with the "long-axis" $(OMoO)_2$ plane, occurs at approximately the same energy as in $Mo_2(O_2CCH_3)_4$. The lack of sensitivity of this 0–0 component to ligand substituents (CH_3 or CF_3) rules out any interpretation based on charge transfer to or from the ligand π or π^* levels; that is, it is apparent that the transition is metal localized. The degeneracy of the parent excited state suggests a transition to or from a metal–metal π or π^* orbital. Considering the energies of the metal δ and δ^* orbitals,[23] the transition must be $\delta \rightarrow \pi^*$ or $\pi \rightarrow \delta^*$. The latter assignment may be rejected, as $X\alpha$ calculations[23] on $Mo_2(O_2CH)_4$ have indicated that $\delta \rightarrow \pi^*$ falls below $\pi \rightarrow \delta^*$ and, more importantly, that *only* the former transition is metal localized (% Mo: δ, 89; π^*, 96; π, 65; δ^*, 86). We conclude, therefore, that the 23 000-cm^{-1} system in $Mo_2(O_2CCH_3)_4$ is attributable to the transition $^1A_{1g} \rightarrow {}^1E_g$ ($\delta \rightarrow \pi^*$), which is low symmetry split by about 275 cm^{-1}.

It has been shown[24] that the $\delta \rightarrow \pi^*$ band in the electronic spectrum of $Re_2Cl_8^{2-}$ lies only 3700 cm^{-1} above that attributable to $\delta \rightarrow \delta^*$. Apparently, in the molybdenum(II) carboxylates, splitting of the δ levels has increased to the point where $\delta \rightarrow \pi^*$ is now slightly lower in energy than $\delta \rightarrow \delta^*$, and it has been suggested[23] that the latter transition in $Mo_2(O_2CH)_4$ be associated with an intense shoulder at 30 800 cm^{-1}. The difference in the spectral behavior of $Mo(O_2CH)_4$ and $Mo_2Cl_8^{4-}$ may be related to the fact[23] that the metal–metal bond distance is 0.05 Å shorter in the former complex, but further studies will be needed to clarify why the $\delta \rightarrow \delta^*$ splitting is affected more than $\delta \rightarrow \pi^*$.

Acknowledgment. We thank George Rossman for assistance with certain experiments. Professors F. A. Cotton, D. S. Martin, and J. G. Norman, Jr., are acknowledged for helpful discussions. W.C.T. held an IBM Fellowship during 1976–1977. This research was supported by the National Science Foundation.

Registry No. $Mo_2(O_2CCH_3)_4$, 14221-06-8; $Mo_2(O_2CCF_3)_4$, 36608-07-8; $Mo_2(O_2CCD_3)_4$, 61483-82-7; $Mo_2(O_2CH)_4$, 51329-49-8; $K_4Mo_2Cl_8$, 25448-39-9.

References and Notes

(1) To whom correspondence should be addressed.
(2) C. D. Cowman and H. B. Gray, *J. Am. Chem. Soc.*, **95**, 8177 (1973).
(3) A. P. Mortola, J. W. Moskowitz, N. Rösch, C. D. Cowman, and H. B. Gray, *Chem. Phys. Lett.*, **32**, 283 (1975).
(4) J. G. Norman and H. J. Kolari, *J. Am. Chem. Soc.*, **97**, 33 (1975).
(5) L. Dubicki and R. L. Martin, *Aust. J. Chem.*, **22**, 1571 (1969).
(6) F. A. Cotton, D. S. Martin, T. R. Webb, and T. J. Peters, *Inorg. Chem.*, **15**, 1199 (1976).
(7) F. A. Cotton, D. S. Martin, P. E. Fanwick, T. J. Peters, and T. R. Webb, *J. Am. Chem. Soc.*, **98**, 4681 (1976).
(8) T. A. Stephenson, E. Bannister, and G. Wilkinson, *J. Chem. Soc.*, 2538 (1964).
(9) F. A. Cotton and J. G. Norman, *J. Coord. Chem.*, **1**, 161 (1971).
(10) J. G. Norman and H. J. Kolari, *J. Chem. Soc., Chem. Commun.*, 649 (1975).
(11) J. V. Brencic and F. A. Cotton, *Inorg. Chem.*, **9**, 351 (1970).
(12) F. A. Cotton, A. C. Mester, and T. R. Webb, *Acta Crystallogr., Sect. B*, **30**, 2768 (1974).
(13) The relatively small $\delta \rightarrow \delta^*$ oscillator strength is in line with theoretical expectations for such a one-electron N → V transition (R. S. Mulliken, *J. Chem. Phys.*, 7, 20 (1939)). The effective dipole moment, Q, is given by $Q \simeq Sr$ in the model (valence bond) that is particularly appropriate for small orbital overlaps. The oscillator strength, f_V^N, is found to be $1.096 \times 10^{11} \nu S^2 r^2$, where S is the orbital overlap, r the internuclear distance in cm, and ν the transition energy in cm^{-1}. Using wave functions for Mo^+ (H. Basch and H. B. Gray, *Theor. Chim. Acta*, **4**, 367 (1966)), we find a δ overlap of 0.10 for $r = 2.14 \times 10^{-8}$ cm, which in turn predicts an oscillator strength of 0.01 for a $\delta \rightarrow \delta^*$ transition at 19 300 cm^{-1}.
(14) J. B. Birks, "Photophysics of Aromatic Molecules", Wiley-Interscience, New York, N.Y., 1970, pp 87–88.

(15) G. W. Robinson and R. P. Frosch, *J. Chem. Phys.*, **38**, 1187 (1963).
(16) G. Herzberg, "Molecular Spectra and Molecular Structure", Vol. III, Van Nostrand-Reinhold, New York, N.Y., 1966, pp 134–136.
(17) C. J. Ballhausen, "Introduction to Ligand Field Theory", McGraw-Hill, New York, N.Y., 1962, pp 185–186.
(18) W. K. Bratton, F. A. Cotton, M. Debeau, and R. A. Walton, *J. Coord. Chem.*, **1**, 121 (1971).
(19) Reference 16, p 140.
(20) J. San Filippo and H. J. Sniadoch, *Inorg. Chem.*, **12**, 2326 (1973).
(21) E. I. Solomon and C. J. Ballhausen, *Mol. Phys.*, **29**, 279 (1975).
(22) K. Nakamoto, "Infrared Spectra of Inorganic and Coordination Compounds", 2nd ed, Wiley, New York, N.Y., 1970, p 223.
(23) J. G. Norman, H. J. Kolari, H. B. Gray, and W. C. Trogler, *Inorg. Chem.*, in press.
(24) W. C. Trogler, C. D. Cowman, H. B. Gray, and F. A. Cotton, *J. Am. Chem. Soc.*, in press.

Contribution from the Department of Chemistry, Louisiana State University, Baton Rouge, Louisiana 70803

Low-Temperature Absorption and Magnetic Circular Dichroism of Gold(III) Tetrachloride Ions in Dicesium Sodium Yttrium Hexachloride

ROBERT W. SCHWARTZ

Received September 10, 1976 AIC60678X

The absorption spectrum at room temperature, liquid nitrogen temperature, and liquid helium temperature and the magnetic circular dichroism at liquid helium temperature have been measured for $AuCl_4^-$:Cs_2NaYCl_6. The results can be explained by assuming the gold ion is present as the tetrachloroaurate ion plus two trans chlorides, i.e., at a site of "six-coordinate" D_{4h} symmetry instead of the O_h symmetry present in the undoped material. No obvious effects of the two trans chlorides were observed. The two observed absorptions are allowed ligand-to-metal charge-transfer transitions. They are assigned, in order of increasing energy, as $^1A_{1g} \rightarrow {}^1E_u(\pi) + {}^1A_{2u}$ and $^1A_{1g} \rightarrow {}^1E_u(\sigma)$. The transitions to $^1E_u(\pi)$ and $^1A_{2u}$ overlap but can be distinguished in MCD by their oppositely signed B terms. For $^1E_u(\pi)$ $|\mu_z| = 0.2$ ($\pm 100\%$) μ_B. Considerable fine structure was observed at the lowest temperatures in the $^1E_u(\pi)$ transition and an assignment is proposed. This structure arises from (1) vibronic transitions involving vibrations of the $AuCl_4^-$ moiety and (2) multiple quanta transitions of lattice vibrations.

Introduction

Square-planar transition metal complexes, via their absorption spectra, have long been a fertile testing ground for molecular orbital theory.[1] Depending on the combinations of metal and ligand any, or all, of the following types of transitions can be observed: d–d, ligand-to-metal charge transfer, metal-to-ligand charge transfer, and intraligand transitions. Most optical studies of these compounds have taken place in solution;[2] however there has recently been some single-crystal work at low temperatures.[3] In addition to allowing the polarization characteristics of the various absorptions to be measured the use of single crystals at low temperatures should provide for improved resolution due to line width narrowing. Unfortunately in most D_{4h} cases this narrowing is insufficient to completely resolve the observed transitions.[4] In only a few cases, all involving d–d transitions, has any vibrational structure been seen. This structure has always been a progression in the totally symmetric (a_{1g}) vibration built on false origins.[3] Thus no information about the excited-state energies of any vibrations except a_{1g} is available.

One example is the absorption and luminescence spectra of $PtCl_4^{2-}$:Cs_2ZrCl_6.[5] The substitution of the divalent platinum ion for the tetravalent zirconium ion is accompanied by the loss of two trans chlorides as charge compensation. This puts the Pt^{2+} ion on a site of D_{4h} symmetry. The net result is that the square-planar $PtCl_4^{2-}$ moiety replaces the octahedral $ZrCl_6^{2-}$ species. The spectra were interpreted primarily using the model of isolated $PtCl_4^{2-}$ molecules and only minimal interaction with the lattice. In that study also only d–d transitions were reported. The major advantage found for this type of substitution was a sharpening of the vibrational structure compared to, for example, pure K_2PtCl_4.

All previous optical studies of gold(III) complexes have been at room temperature.[6] It is well established that the two lowest energy charge-transfer absorptions are $^1A_{1g} \rightarrow {}^1A_{2u} + {}^1E_u(\pi)$ and the $^1A_{1g} \rightarrow {}^1E_u(\sigma)$, respectively. The $^1A_{2u}$ and $^1E_u(\pi)$ terms have not previously been resolved for the Au^{3+} ion. Gold(III)–ligand vibrational energies have been well studied. In particular the ground-state vibrational energies in $AuCl_4^-$ of all modes, except the b_{2u} vibration, have been reported.[7] In addition to solution studies the solid-state spectra of $MAuCl_4$ have been studied for various M^+ cations to determine the dependence of the vibrational energies on M^+. For all cases the maximum change observed was ~8%.

The electronic spectra of impurity centers in solids can provide information about the impurity, the host lattice, and the interaction between them. In an attempt to obtain information on each of the above areas and as a part of a continuing study[8] of the elpasolite hexachlorides $Cs_2NaLnCl_6$, Ln = trivalent lanthanide or yttrium(III), the absorption and magnetic circular dichroism (MCD) spectra of $AuCl_4^-$:Cs_2NaYCl_6 have been measured and are reported herein. Previous work involving $Cs_2NaLnCl_6$ has concerned itself with several different types of optical transitions which in turn have monitored different vibrations in the crystal. Ligand-to-metal charge-transfer transitions have been measured for Re^{4+}:Cs_2NaYCl_6[8c] and some gerade vibrations observed. Transitions of this type are also considered in this work.

The d–d transitions in Cr^{3+}:Cs_2NaYCl_6 have been reported.[8e] In addition to several magnetic dipole induced transitions (origins) these Laporte-forbidden transitions gained intensity primarily via vibronic coupling with higher energy ungerade terms. The vibrations observed were assigned as ungerade modes within the model of an octahedral $CrCl_6^{3-}$ moiety interacting only very weakly with the surrounding lattice. In addition to these ungerade modes progressions in a_{1g} and e_g $CrCl_6^{3-}$ moiety vibrations were also observed. This behavior is very different from that observed in the Laporte-forbidden f–f transitions in $Cs_2NaEuCl_6$,[8d] $Cs_2NaPrCl_6$,[9] $Cs_2NaTbCl_6$,[10a] and $Cs_2NaTmCl_6$.[10] In those and other lanthanide cases a density of vibrational states over the entire Brillouin zone was observed. For the most part the vibrations observed corresponded to ungerade modes at the zone center (Γ point). However the contrast between the f–f transitions "sampling" the vibrations of the entire lattice and the d–d transitions seeming to be located totally within the $CrCl_6^{3-}$ moiety is remarkable.

Some of the electric dipole allowed f → d transitions in Ce^{3+}:Cs_2NaYCl_6 have also been reported.[8a] These were the $^2F_{5/2}(E''_u) \rightarrow {}^2T_{2g}(U'_g + E''_g)$ transitions. Aside from the